ISSN 2070-2051, Protection of Metals and Physical Chemistry of Surfaces, 2016, Vol. 52, No. 6, pp. 1086–1092. © Pleiades Publishing, Ltd., 2016.

PHYSICOCHEMICAL PROBLEMS OF MATERIALS PROTECTION

Study of Inhibition Effect of Carboxylic Salt Derivative on Corrosion of C1010 Carbon Steel in Saline Solution[1]

Mehdi Salih Shihab*, Abbas Hadi Alshukrawi, and Wedad Hamad Aldahhan

Al-Nahrain University, College of Science, Department of Chemistry, Al-Jadrya, Baghdad, Iraq

**e-mail: mehdi_shihab@yahoo.com*

Received August 21, 2015

Abstract—In the present work, sodium 4-[(4-formylbenzylidene) amino] benzoiate (**4**) was synthesized and its structure was confirmed using spectroscopic techniques. Prepared compound was successfully applied as a corrosion inhibitor for C1010 carbon steel in 3.5% NaCl solution at 25°C. Different electrochemical measurements such as linear polarization resistance (LPR), potentiodynamic polarization (PDP), and electrochemical impedance spectroscopy (EIS) were used to evaluate the suggested inhibitor (**4**). The results of different electrochemical measurements show that inhibition efficiencies obtained from EIS curves are in consistence with the results of potentiodynamic polarization and LPR measurements due to increase corrosion inhibition efficiency by increasing the concentration of organic inhibitor (**4**). Semi-empirical calculations with PM3 method were used to find relationship between molecular structure and inhibiting effect of suggested inhibitor (**4**).

DOI: 10.1134/S2070205116060174

1. INTRODUCTION

Corrosion is defined as the deterioration of a material due to reaction with its environment. Wet, saline and aerated conditions make steel to be exposed to corrosion process on the surface. This harmful attack can cause defect in the mechanical, physical and chemical properties of metal. Therefore, protection methods should be developed to reduce the damage effects of the metal. Organic inhibitors are very effective way for the reducing of corrosion of metals and alloys due to generate a thin film that controls and prevents access of corrosive agents to the metal surface. The organic inhibitors that used for control corrosion of steel are organic compound containing nitrogen, oxygen and/or sulphur atoms [1–4].

Inhibitors have very wide application in a variety of industrial applications such as cooling systems, refinery units, pipelines, chemicals, oil and gas production units, boilers and water processing, paints, pigments, lubricants, etc. [5]. In acidic media, Schiff base derivates as corrosion inhibitor were used for various metals and alloys such as carbon steel, aluminum and copper [6–10]. Stable complexes could be formed between Schiff base ligands metal ions [11]. Therefore, these compounds have wide applications and large potential in corrosion and protection area. Schiff base, namely N-(2-hydroxybenzylidene) thiosemicarbazide was investigated as inhibitor for carbon steel in saline water at different concentrations [12].

In the present work, we studied the inhibition properties of sodium 4-[(4-formylbenzylidene) amino] benzoiate for the corrosion of C1010 carbon steel in 3.5% NaCl solution. Linear polarization resistance (LPR), potentiodynamic polarization (PDP), and electrochemical impedance spectroscopy (EIS) were used for investigating the corrosion behavior. Semi-empirical calculations were used to form molecular structure model to study inhibition effect of suggested inhibitor.

2. EXPERIMENTAL

2.1. Materials and Synthesis

All chemical materials were used as received without further purification. Pyridinium bromide derivative inhibitor, namely: sodium 4-[(4-formylbenzylidene) amino] benzoiate (**4**) was synthesized by two steps, as follows:

– Preparation of 4-[(4-formylbenzylidene) amino] benzoic acid (**3**): A mixture of terephthalaldehyde (**1**) (0.01 mol), abs. ethanol (20 mL) and 4-aminobenzoic acid (**2**) (0.01 mol) with a few drops of glacial acetic acid was refluxed for 6 h. After cooling to room temperature, the precipitate was filtered and dried. The product was crystallized from ethanol [13]. Yield 85%, m.p. > 390°C. FTIR (ZnSe) cm^{-1}, 3300–2500 (O–H), 3100 (C–H, aromatic), 2720 (H–C=O), 1675 (C=O), 1603 (C=N), 1589 (C=C). ^{1}HNMR (600MHz,

[1] The article is published in the original.

DMSO-d_6) δppm: 7.3–8.2(m, C–H, aromatic) and 8.6 (m, CH=N), 10.1 (s, 1H, H–C=O).

– Preparation of compound (**4**): A mixture of compound (**3**) (0.01 mol), distilled water (30 mL) and NaOH (0.0105 mol) was stirred under gentle heating for 10 min. The solvent was removed until dried product. Yield 96%, m.p. = 310°C (dec.). ^{1}HNMR (600MHz, D_2O) δppm: 7.3–8.2 (m, C–H, aromatic) and 8.6 (m, CH=N), 10.1 (s, 1H, H–C=O). The chemical steps that included preparing the suggested Inhibitor (**4**) are shown in Scheme 1.

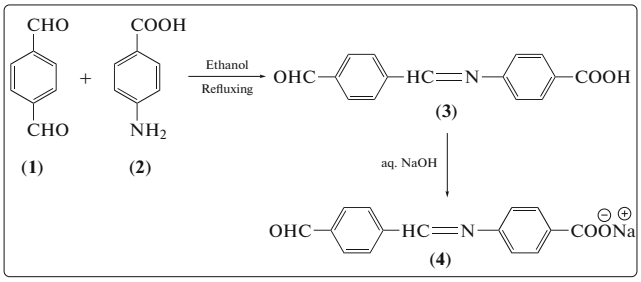

Scheme 1. Preparation scheme of carboxylic acid salt derivative (4).

2.2. Test Material

The experiments were carried out with C1010 carbon steel specimens (C%, 0.1; Mn%, 0.45; P%, 0.04; S%, 0.05; Fe%, balance). Square specimens with an exposed area of (1 cm^2) were encapsulated in epoxy resin as a working electrode. The surface of working electrodes were wet polished using emery papers up to 1500 grit and then cleaned with deionized water, alcohol, and finally acetone.

2.3. Test Solution

The saline solutions with 3.5% NaCl were prepared by using deionized water. The concentrations range of inhibitor employed was 0.003–0.018 M.

2.4. Electrochemical Measurements

Corrosion behavior was studied by means of electrochemical techniques such as linear polarization resistance (LPR), potentiodynamic polarization (PDP), and electrochemical impedance spectroscopy (EIS). Polarization curves were recorded at a constant sweep rate of 1 mV/s at the interval from –500 to +500 mV respect to the open circuit potential (OCP). The experiments were designed with a conventional three- electrode cell assembly using Potentiostat/Galvanostat/ZRA (Gamry, Reference 600). The working electrode was C1010 carbon steel. A saturated calomel electrode (SCE) was used as the reference electrode and platinum gauze was employed as the counter electrode. The linear polarization resistance was carried out at ±0.015 V with respect to the corrosion potential at a sweep rate of 0.125 mV s^{-1}. The polarization was carried out at cathodic potential of –0.3 V to an anodic potential of +0.3 V with respect to the corrosion potential at a sweep rate of 1 mV s^{-1}. The Tafel plots of anodic and cathodic curves were extrapolated to corrosion potential to get the values of corrosion current, *I*corr. Electrochemical impedance measurements were carried out at open circuit potential after immersing the mild steel specimen in experimental solution in the frequency range of 10 kHz to 0.1 Hz. Applied voltage of sinusoidal wave was 10 mV. All of electrochemical measurements were carried out after the open circuit potential of the system was stabilized (after 3–4 hours immersion time). In addition, tests were conducted at room temperature (25°C).

The Gamry device was controlled by a desktop computer with DC105 DC Corrosion Software License and EIS300 Electrochemical Impedance Software License. Data analysis achieved by Gamry echem analyst version 6.24.

3. RESULTS AND DISSCUSSION

The results of corrosion rate and inhibition efficiency that were obtained from LPR measurements for C1010 carbon steel in 3.5% NaCl solution in the presence of different inhibitor (**4**) concentrations at temperature 25°C are depicted in Fig. 1 and summarized in Table 1.

The percentage inhibition efficiency (IE (%)) was calculated using the relationship:

$$\mathrm{IE}\,(\%) = \frac{W_{\mathrm{corr}} - W_{\mathrm{corr\,(inh)}}}{W_{\mathrm{corr}}}. \qquad (1)$$

Where W_{corr} and $W_{\mathrm{corr\,(inh)}}$ are the corrosion rates of carbon steel in the absence and presence of inhibitor, respectively.

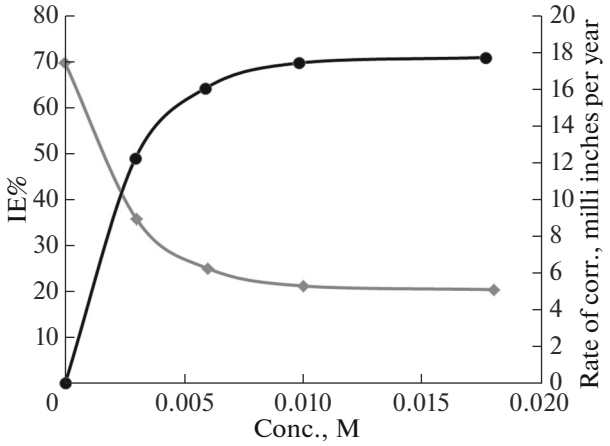

Fig. 1. Effect of inhibitor (**4**) concentrations on corrosion rate and inhibition efficiency for C1010 carbon steel in 3.5% NaCl solution at temperature 25°C.

Table 1. Rate of corrosion, inhibition efficiency, surface coverage (θ) and standard free energy of adsorption for C1010 carbon steel in 3.5% NaCl solution in different inhibitor (**4**) concentrations at temperature 25°C by using LPR measurements

No	Inhibitor concentration, M	Rate of corrosion, milli-inches/year	IE, %	θ	ΔG°_{ads}, kJ/mol
1	Uninhibited	17.45	–	–	
2	0.003	8.92	48.9	0.489	
3	0.006	6.23	64.2	0.642	–25.8 ($R^2 = 0.998$)
4	0.010	5.28	69.7	0.697	
5	0.018	5.08	70.9	0.709	

Table 2. Electrochemical polarization parameters for C1010 carbon steel in 3.5% NaCl solution containing different concentrations of inhibitor (**4**) at 25°C

No	Inhibitor concentration, M	Tafel slopes, mV/decade		E_{corr}, mV	i_{corr}, μA/cm^2	Inhibition efficiency, %[a]
		β_a	β_c			
1	Uninhibited	223.3	120.5	–766	14.1	–
2	0.003	78.7	104.0	–644	7.9	44.0
3	0.006	102.6	168.0	–574	6.5	53.9
4	0.010	97.7	203.5	–503	5.8	58.8
5	0.018	87.2	154.9	–474	4.0	71.6

[a] $IE\% = 1 - (i_{corr\,(inh)}/i_{corr(uninh)})$.

The interaction between the organic compounds and metal surfaces can be explained from the basic information of adsorption isotherms. Specifically, the degree of surface coverage values (θ) at different inhibitor concentrations in 3.5% NaCl solution was achieved by the relationship (θ = IE (%)/100) (see Table 1) at 25°C and tested with Langmuir isotherm relationship [14]:

$$C/\theta = 1/K_{ads} + C. \quad (2)$$

Where K_{ads} is the equilibrium constant of the adsorption process, C is molar concentration of inhibitor in water in unit M.

According to the Langmuir isotherm, K_{ads} values can be calculated from the intercepts of the straight line of plotting C/θ versus C. Here, K_{ads} is related to the standard free energy of adsorption, ΔG°_{ads}, with the following equation [14]:

$$K_{ads} = \frac{1}{55.5}\exp\left(-\frac{\Delta G^{\circ}_{ads}}{RT}\right). \quad (3)$$

The value 55.5 is the molar concentration of water in the solution in M unit. In Table 1, the value of standard free energy of adsorption is negative (–25.8 kJ/mole). This indicates that the process of adsorption of the suggested inhibitor (**4**) was spontaneous process on the carbon steel surface at 25°C, and that given sense for remarkable interaction between suggested inhibitor and the metal surface. Here, adsorbed molecule moves closer to the surface of metal that makes electrons of organic molecule start to overlap with that of the surface atoms which causes physisorption for suggested inhibitor [15, 16].

The polarization parameters E_{corr}, i_{corr}, anodic and cathodic Tafel slopes (β_a, β_c) obtained from polarization measurements are given in the Table 2. It is clear that the values of corrosion current density decreases significantly with increasing of carboxylic salt derivative (**4**) concentrations. Corrosion potential values decrease with increase in the concentration of inhibitor (**4**). The change in the values of corrosion current density and corrosion potential in different concentrations of carboxylic salt derivative reflected positively on the percentage inhibition efficiencies. It is evident that increasing inhibitor concentrations leads to accumulating layers of pyridinium salt caused reducing in the rate of corrosion, and then increasing the percentage corrosion inhibition efficiency. However, the accumulation of molecules that adsorbed is given additional resistance to corrosion of the metal in addition to occupying reactive sites directly. We believed that higher corrosion inhibition efficiency in suggested inhibitor (**4**) is attributed to the presence of delocalized π-electrons, negative charge on oxygen atom and lone pair of electrons on nitrogen atom. Polarization curves for carbon steel in 3.5% NaCl solution at different inhibitor concentrations at 25°C are shown in Fig. 2. In addition, the β_a and β_c values for the inhibitor (see Table 2) were found to be changed with inhibitor concentration, which indicates that the inhibitor affected both the anodic and the cathodic reactions. Further-

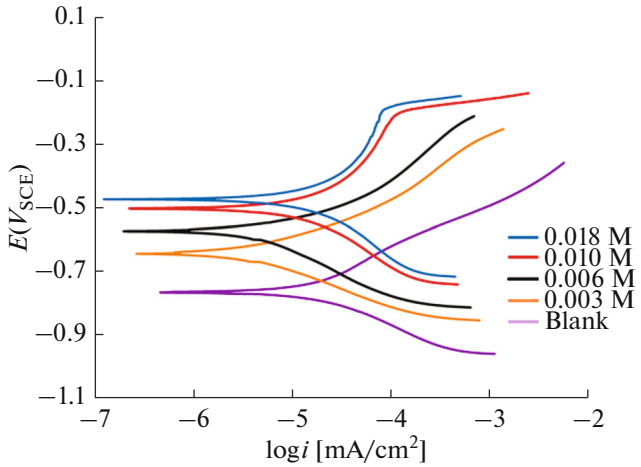

Fig. 2. Effect of carboxylic acid salt derivative (**4**) concentrations in the polarization curves for C1010 carbon steel in 3.5% NaCl solution at 25°C.

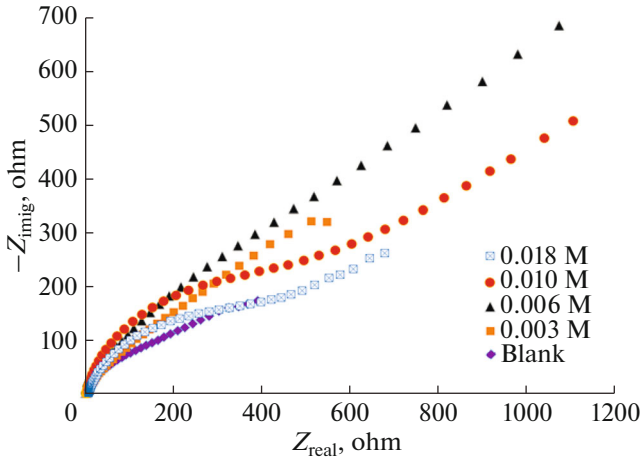

Fig. 3. EIS data in the Nyquist format for C1010 carbon steel in uninhibited and inhibited 3.5% NaCl solutions at 25°C.

more, a positive shift was observed (see Table 2) in the E_{corr} values in the presence of different concentrations of inhibitor (**4**), suggesting that organic inhibitor behaves as a type of anodic inhibitor [17, 18].

The impedance Nyquist plots of C1010 carbon steel in uninhibited and inhibited 3.5% NaCl solutions using different concentrations of carboxylic acid salt derivative (**4**) are shown in Fig. 3. It is clear from Fig. 3 that the protection response of carbon steel was modified in the presence of different concentrations of compound (**4**). It can be concluded that an increase in the surface metal impedance has happened with the increase in the inhibitor concentration. Similar shape of Nyquist plots were depicted that corrosion process followed the same mechanism of corrosion inhibition and dissolution [19]. We can recognize that Nyquist plots are not completely semicircles due to frequency dispersion which could be due to roughness and inhomogeneities of the working electrode surface because of corrosion attack [20, 21]. Also Nyquist plots showed that the diagram of the capacitive loop becomes larger in the presence of inhibitor in solution than that in the absence of inhibitor due to increase the impedance of inhibited substrate with increasing the inhibitor concentration. Adsorption of the inhibitor on the metal surface caused changing in its homogeneity, and then changing in the impedance behavior of solid metal electrodes [22, 23].

Bode modulus diagrams, Fig. 4a, show the ascending trend of low frequency impedance values is obviously seen with increasing the concentrations of carboxylic acid salt derivative (**4**) in 3.5% NaCl solutions. An important idea can be taken from the Bode phase plots, Fig. 4b, is that the more concentration of inhibitor results the higher maximum phase angle, reflecting a capacitive behavior which is related to the increase of polarization resistance in the presence of inhibitor. The tendency of AC current to pass through the resistor in the circuit leads to a drop in the phase angle. Hence, the system exhibiting higher resistance can be characterized by higher phase angle.

Figure 5 show the equivalent circuit, R_{soln} is the solution resistance; R_{po} is the charge transfer resistance; and R_{cor} is the film resistance. C_c and C_{cor} are the constant phase elements (CPEs). C_c is the double-layer capacitance at the film-solution interface and C_{cor} is the capacitance of the film.

In many cases of the electrochemical process, it could be represented non-ideal capacitance response by using the constant phase element (CPE) instead of a pure capacitance. The symbol *n or m* is a mathematical expression where $0 \le n \le 1$. If $n = 0$, the impedance is used as a resistance, while it is capacitance when $n = 1$. In other words, when $0 < n < 1$, represents one of the various cases for deviation from the ideal capacitance. These cases of deviation which are related to the surface roughness, adsorption film, porous layer formation [19].

The EIS parameters are fitted of Equivalent circuit model (see Fig. 5) and given in Table 3. The results of Table 3 shows that charge transfer resistance (R_{po}) increases, indicating that the corrosion is decelerated. That's mean; the presence of suggested inhibitor (**4**) decelerates the corrosion of carbon steel. Also, the solution resistance (R_{soln}) increased in the presence of suggested inhibitor (**4**), because the process of releasing metal ions from carbon steel is decreasing, that causes lowering in electrical conductivity. For the film resistance (R_{cor}), these values increase with increasing in suggested inhibitor (**4**) concentrations. Because the developing of protecting film of the surface of carbon steel. The values of n, m supports the idea that surface inhomogeneity during the process of corrosion in the

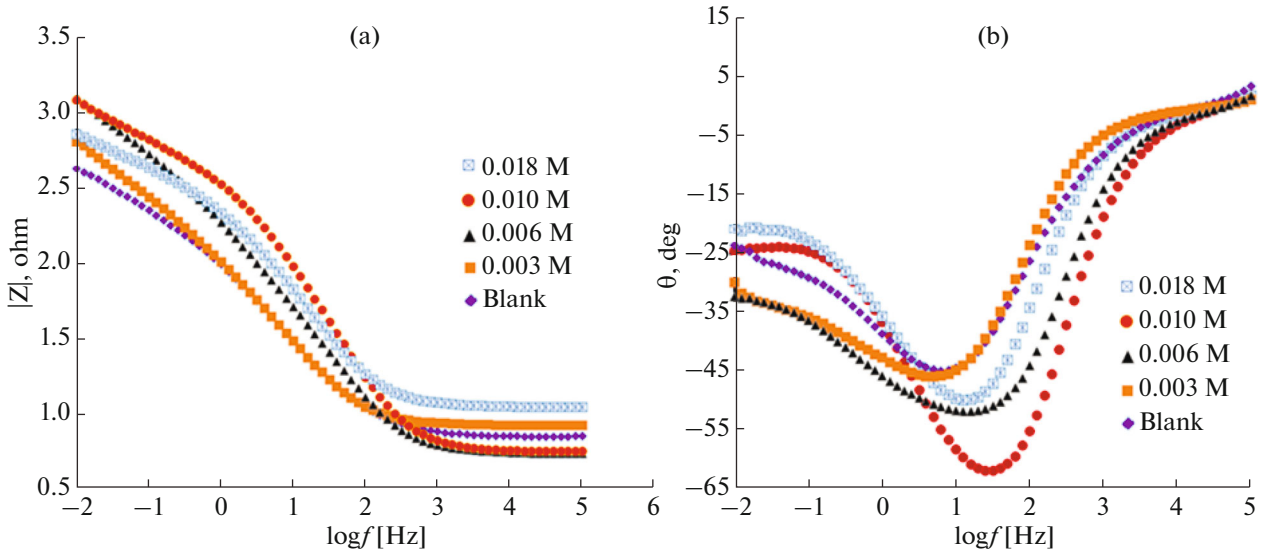

Fig. 4. EIS data in the Bode modulus (a) and Bode phase (b) plots for C1010 carbon steel in uninhibited and inhibited 3.5% NaCl solutions at 25°C.

absence and presence of suggested inhibitor (**4**). C_{cor} values are decreased as soon as the inhibitor is added. The continuous inhibitor adsorption on the metals surface blocks the active surface decreasing C_{cor} and increasing R_{cor} (see Table 3). C_c values are decrease with increasing inhibitor (**4**) due to decelerate the corrosion process and m value remained almost constant suggesting the formation of a homogenous inhibitor film [24]. R_{po} can be associated with the pore sized of the inhibitor film [25]. The increase of R_{po} could be related to the formation of a more compact film (see Table 3). Inhibition efficiency values in Table 3 shows enhancement for protection carbon steel metal by increasing suggested inhibitor (**4**).

Also, Fig. 6 shows comparison images among specimens of C1010 carbon steel in 3.5% NaCl solution at 25°C after the measurements process which confirmed the effect of carboxylic acid salt derivative (**4**) as inhibitor.

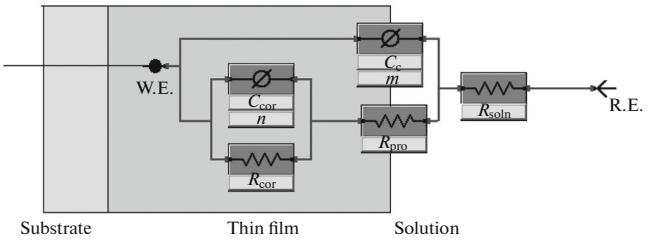

Fig. 5. Equivalent circuit.

Finally, to study the relationship between molecular structure and inhibiting effect of the suggested inhibitor (**4**), molecular orbitals of semi-empirical calculations with PM3 method were used [26]. Semi-empirical calculations were achieved using the Hyperchem Program [27] with complete geometry optimization. The adsorption of the inhibitor on the metal surface can be considered on the basis of donor-acceptor. Quantum calculations were performed for

Table 3. Impedance data for C1010 carbon steel in 3.5% NaCl solution for various concentrations of carboxylic acid salt derivative (**4**) at 25°C

Inhibitor Conc., M	R_{soln}, ohm cm^2	$R_{cor.}$, ohm cm^2	R_{po}, ohm cm^2	C_{cor}, S.s^n cm^{-2} × 10^3	n	C_c, S.s^m cm^{-2} × 10^3	m	IE%[a]
Blank	7.1	1093	154	7.4	0.44	1.96	0.69	
0.003	8.2	2218	315	2.0	0.33	1.32	0.78	50.7
0.006	9.3	4291	167	3.0	0.40	0.93	0.79	74.5
0.010	5.6	6509	240	2.3	0.31	0.28	0.84	83.2
0.018	8.7	7771	222	1.7	0.32	0.25	0.84	86.0

[a] IE% = [1 − R_{cor} (uninh)/R_{cor}(inh)] × 100

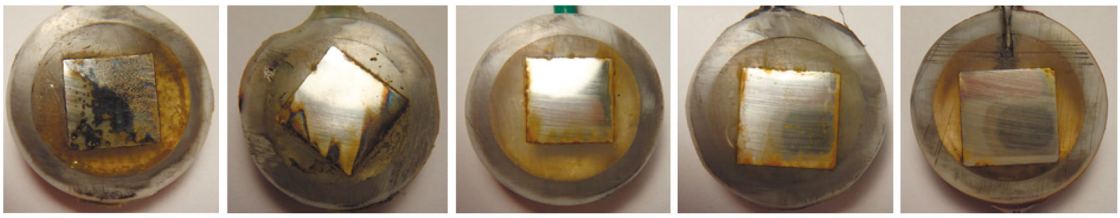

Fig. 6. Specimen images of C1010 carbon steel in 3.5% NaCl solution in the absence and presence of inhibitor (**4**).

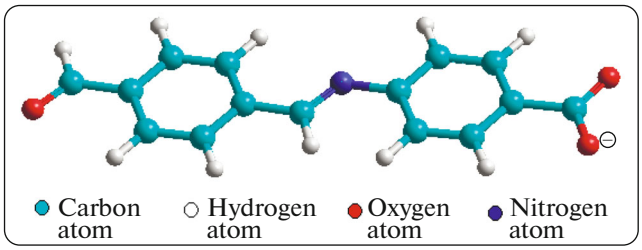

Fig. 7. More energetically stable conformations of carboxylic acid salt derivative (**4**) with PM3 method.

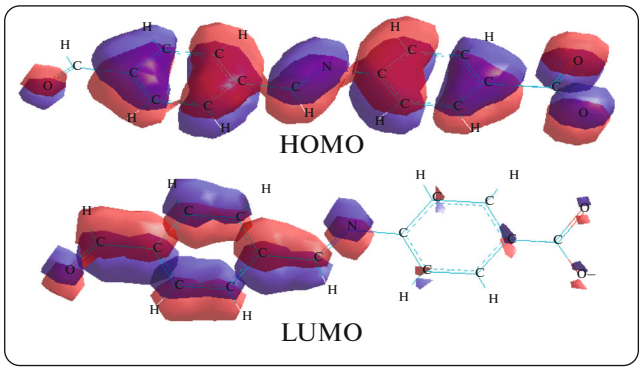

Fig. 8. The frontier molecular orbital density distributions (HOMO and LUMO) for carboxylic acid salt derivative (**4**) by using PM3 method.

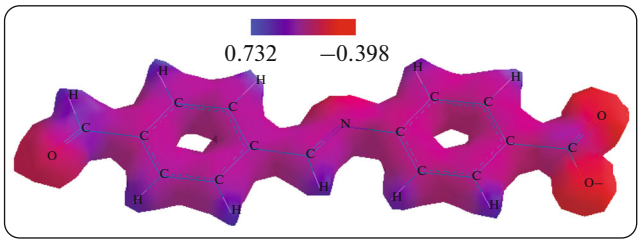

Fig. 9. Electrostatic potential maps for carboxylic acid salt derivative (**4**) by using PM3 method.

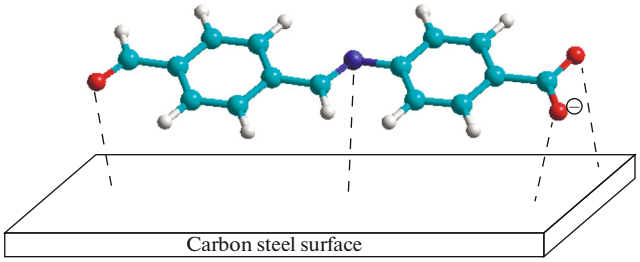

Fig. 10. Suggested physisorption of carboxylic acid salt derivative (**4**) on C1010 carbon steel surface.

carboxylic acid salt derivative (**4**) using more energetically stable conformations without any symmetry constraints in the gas phase at 25°C, (see Fig. 7). The calculated chemical parameters are given in Table 4 (energies of E_{HOMO} and E_{LUMO}, energy gap (ΔE) and other indices) are resulted of optimized molecular modeling system of suggested inhibitor by PM3 method. The PM3 method for estimation HOMO and LUMO isosurfaces for suggested inhibitor are shown in Fig. 8. It's clear from Fig. 8 that the repartition density of the HOMO and LUMO is preferentially localized on nitrogen (N), oxygen (O) atoms and π-system of molecular modeling system of carboxylic acid salt derivative (**4**). Inhibition efficiency can be correlated to the energy levels of HOMO and LUMO and the difference between them and the smaller value of ΔE of an inhibitor makes its inhibition efficiency higher because the excitation energy gap is more polarizable and is generally associated with a high chemical reactivity [28].

The inhibitor (**4**) has a high value of dipole moment due to existence of hetero atoms (N, O) and positively charge of the nitrogen atom of pyridine ring. This polarity of inhibitor molecule could be a good factor to improve the dipole–dipole interaction between organic molecule and metal steel surface and then to enhance corrosion inhibition [29].

Electrostatic potential maps for organic inhibitor model depicted in Fig. 9. This Figure shows the non-uniform distribution of electron density and concentration of negative charges on the atoms of N (C=N) and O (C=O, COO^-) for organic inhibitor (**4**) model, which explains a high value of the calculated dipole moment (see Table 4).

Complete geometry optimization of carboxylic acid salt derivative as a molecular modeling system results full-planarity configuration (see Table 4),

Table 4. Quantum calculation results of carboxylic acid salt derivative (**4**) by using PM3 method

Inhibitor: carboxylic acid salt derivative
HOMO (eV): −4.8210
LUMO (eV): 0.8650
Energy gap ($\Delta E = E_{HOMO} - E_{LUMO}$) (eV): −5.6860
μ (Debye): 23.29
Planarity: planar

which improved the inhibition efficiency by making the active sites (N (C=N) and O (C=O, COO^-) atoms) closer to the surface of metal and that in turn improved the physisorption at high concentrations. Figure 10 shows suggested physisorption mechanism of carboxylic acid salt derivative (**4**) on the surface of metal.

For this work, we can conclude that molecular modeling system is an appropriate tool to create correlation between theoretically calculated properties and experimentally determined inhibition efficiencies for corrosion process of carboxylic acid salt derivative (**4**) in 3.5% NaCl solution at 25°C.

4. CONCLUSION

Carboxylic acid salt derivative was prepared and its structure was confirmed physical and spectroscopic techniques. Various concentrations of carboxylic acid salt derivative were used successfully as corrosion inhibitors for C1010 carbon steel in 3.5% NaCl solution at 25°C. The results of corrosion rate and inhibition efficiency obtained from LPR technique indicate that the carbon steel corrosion was reduced in the presence of the suggested inhibitor. The polarization parameters such as corrosion current density decreased significantly with increasing of the carboxylic acid salt derivative concentration. The inhibition efficiencies obtained from EIS curves were in consistence with the results of potentiodynamic polarization and LPR measurements. A good correlation was found between theoretically calculated properties and experimentally determined inhibition efficiencies for corrosion process of carboxylic acid salt derivative in 3.5% NaCl solution by using molecular orbitals of semi-empirical calculations with PM3 method.

ACKNOWLEDGMENT

The financial support of this work by the U.S. Department of State, with its implementing partner CRDF Global, under the Iraq Science Fellowship Program (ISFP) was gratefully acknowledged.

REFERENCES

1. Abdallah, M., Basim, H. Asghar, Zaafarany, I., and Fouda, A.S., *Int. J. Electrochem. Sci.,* 2012, vol. 7, p. 282.
2. Abdel-Aal, M. and Morad, M.S., *Br. Corros. J.,* 2001, vol. 36, p. 250.
3. Abdallah, M., Meghed, H.E., and Sobhi, M., *Mater. Chem. Phys.,* 2009, vol. 118, p. 111.
4. Abdallah, M., Zaafarany, I., Khairou, K., and Sobhi, M., *Int. J. Electrochem. Sci.,* 2012, vol. 7, p. 1564.
5. Sastri, V., *Corrosion Inhibitors: Principles and Applications,* New York: Wiley-Blackwell, 1998.
6. Li, S., Chen, S., Lei, S., et al., *Corros. Sci.,* 1999, vol. 41, p. 1273.
7. Emregu, K.C. and Atakol, O., *Mater. Chem. Phys.,* 2003, vol. 82, p. 188.
8. Emregu, K.C. and Atakol, O., *Mater. Chem. Phys.,* 2004, vol. 83, p. 373.
9. Emregu, K.C., Kurtaran, R., and Atakol, O., *Corros. Sci.,* 2003, vol. 45, p. 2803.
10. Yurt, A., Ulutas, S., and Dal, H., *Appl. Surf. Sci.,* 2006, vol. 253, p. 919.
11. Kendig, M. and Jeanjaquet, S., *J. Electrochem. Soc.,* 2002, vol. 149, p. B47.
12. Samide, A. and Tutunaru, B., *J. Environ. Sci.,* 2011, vol. 46, p. 1713.
13. Mohite, P.B. and Bhaskar, V.H., *Orbital: Electron. J. Chem.,* 2011, vol. 3, p. 117.
14. Agrawal, R. and Namboodhiri, T., *Corros. Sci.,* 1990, vol. 30, p. 37.
15. Ehteram A. Noor and Aisha H. Al-Moubaraki, *Mater. Chem. Phys.,* 2008, vol. 110, p. 145.
16. Bentiss, F., Lebrini, M., and Lagrenee, M., *Corros. Sci.,* 2005, vol. 47, p. 2915.
17. Chauhan, L.R. and Gunasekaran, G., *Corros. Sci.,* 2007, vol. 49, p. 1143.
18. Hegazy, M.A., *Corros. Sci.,* 2009, vol. 51, p. 2610.
19. Mansfeld, F., Kending, M.W., and Tsai, S., *Corrosion,* 1981, vol. 37, p. 301.
20. Jeyaprabha, C., Sathiyanarayanan, S., Muralidharan, S., and Venkatachari, G., *J. Braz. Chem. Soc.,* 2006, vol. 17, p. 61.
21. Growcock, F.B. and Jasinski, J.H., *J. Electrochem. Soc.,* 1989, vol. 136, p. 2310.
22. Ashassi-Sorkhabi, H., Seifzadeh, D., and Hosseini, M.G., *Corros. Sci.,* 2008, vol. 50, p. 3363.
23. Osman, M.M., Omar, A.M., and Al-Sabagh, A.M., *Mater. Chem. Phys.,* 1997, vol. 50, p. 271.
24. Gao, G. and Liang, C., *Corros. Sci.,* 2007, vol. 49, p. 3479.
25. Lopez, D.A., Simison, S.N., and de Sanchez, S.R., *Corros. Sci.,* 2005, vol. 47, p. 735.
26. Shihab, M.S. and Al-Doori, H.H., *J. Mol. Struct.,* 2014, vol. 1076, p. 658.
27. *HyperChem 2002, Version 7.5,* Gainesville: Hypercube Inc., 2002.
28. Tang, Y., Xiaoyuan, Y., Wenzhong, Y., et al., *Corros. Sci.,* 2010, vol. 52, p. 1801.
29. Gao, G. and Liang, C., *Electrochim. Acta,* 2007, vol. 52, p. 4554.